http://dx.doi.org/10.5012/bkcs.2012.33.2.641

DFT Study for Substitution Patterns of $C_{20}H_{18}X_2$ Regioisomers (X = F, Cl, Br, or OH)

Yong Gyoo Hwang,† Seol Lee, and Kee H. Lee*

*Department of Chemistry, and Nanoscale Sciences and Technology Institute, Wonkwang University, Iksan, Jeonbuk 570-749, Korea. *E-mail: khlee@wonkwang.ac.kr*
†Division of Microelectronics and Display Technology, and Nanoscale Sciences and Technology Institute, Wonkwang University, Iksan, Jeonbuk 570-749, Korea
Received November 30, 2011, Accepted January 25, 2012

We used the hybrid density-functional (B3LYP/6-31G(d,p)) method to analyze the substitution patterns of $C_{20}H_{18}X_2$ derivatives (X = F, Cl, Br, or OH) obtained as disubstituted $C_{20}H_{20}$ cages. Our results suggest that the *cis*-1 regioisomers (1,2-dihalo derivatives) are less stable than the *trans*-1 regioisomers (1,20-dihalo derivatives), whereas in the case of the dihydroxy derivatives, the *cis*-1 regioisomer is more stable than the *trans*-1 regioisomer. This implies that in the dihalo-induced strain cages of $C_{20}H_{18}X_2$, the strain effect would affect the relative energies, while in the dihydroxide, the hydrogen bonds have a stronger effect on the relative energies in *cis*-1 regioisomer than the strain effect do. Thus this supports the experimental result in which the bisvicinal tetrol was of particular preparative-synthetic interest as a substitute for the lacking bisvicinal tetrabromide. Further, the topologies of the HOMO and LUMO characteristics of all $C_{20}H_{18}Cl_2$ and $C_{20}H_{18}Br_2$ regioisomers with the same symmetry are same, but they are different from those of $C_{20}H_{18}F_2$ and $C_{20}H_{18}(OH)_2$. This indicates that the five regioisomers of each $C_{20}H_{20}$ disubstituted derivative will have an entirely different set of characteristic chemical reactions.

Key Words : C_{20} dihydroxide and dihalides, $C_{20}H_{18}X_2$ regioisomers, Hybrid density-functional (B3LYP) calculations, HOMO and LUMO

Introduction

The geometry of fullerenes obeys the isolated-pentagon rule (IPR), which states that the most stable fullerenes are those in which all pentagons (five-membered rings, 5-MRs) are located as far as possible from one another and are surrounded by five hexagons (six-membered rings, 6-MRs).[1,2] However, this rule cannot be satisfied for the smallest fullerene, C_{20} (first synthesized in 2000), which contains 12 5-MRs and no 6-MRs.[3] Therefore, the non-IPR fullerene would be highly reactive owing to the fusion of strained 5-MRs. Because this strain is removed through sp^3-bond-forming reactions of C_{20}, isomeric derivatives of C_{20} could be formed. As the C_{20} cage would be a candidate for fabricating molecular devices, the modification of the structural and electronic properties of $C_{20}H_{20}$ should be of interest to both experimentalists and theoreticians.

Isomerism is a fundamental concept in chemistry, and the term "regioisomer" refers to a type of structural isomer. In the formation of regioisomers, regioselectivity is observed in the chemical reactions of molecules with different orientations or reaction sites. Unlike the regioisomers of C_{20} fullerene derivatives with only 5-MRs, the regioisomers of other types of derivatives, including diadducts of fullerenes with 5- and 6-MRs, have been extensively studied.[4,5] The gas-phase production of $C_{20}Br_2$ and $C_{20}H_2$ has been reported.[6,7] Experimental studies in which the relative stability of $C_{20}H_{18}X_2$ regioisomers was observed are very few. Proton transfer between the –OH groups of two $C_{20}(OH_2)_2$ molecules has previously been examined by *ab initio* molecular orbital calculations.[8] Adducts formed from the parent fullerene C_{20} with C_2H_2 and C_2H_4 have been studied by the B3LYP method; the derivatives $C_{20}(C_2H_2)_n$ and $C_{20}(C_2H_4)_n$ (n = 1-3) exhibit remarkable aromaticity, while $C_{20}(C_2H_2)_4$ and $C_{20}(C_2H_4)_4$ have no spherical aromaticity.[9] In addition, we reported that the five bond-stretched isomers of the C_{20} dication could be verified by performing addition reactions and analyzing the highest occupied molecular orbital (HOMO) and the lowest unoccupied molecular orbital (LUMO) maps.[10]

Recently, the planarity of benzene was analyzed by various theoretical methods, and the B3LYP/6-31G(d,p) calculation was found to be suitable for simulating the experimentally determined structure of benzene.[11]

Although many calculations for the parent C_{20} cage[9] as well as $C_{20}H_{20}$ dodecahedrane[12] and $C_{20}F_{20}$ perfluorododecahedrane,[13,14] have been reported, to the best of our knowledge, no calculations of the full optimization of disubstituted $C_{20}H_{18}X_2$ regioisomers (X = F, Cl, Br, or OH) at the level of B3LYP/6-31G(d,p) have been reported. In this study, we determined the relative energies, electronic properties, and atomic structures of $C_{20}H_{18}X_2$ regioisomers having the same spin state. Even though the predominant electronic configurations of the regioisomers are similar, the HOMO and LUMO maps between regioisomers are found to be different. This suggests that different exohedral complexes may undergo a distinct set of characteristic chemical reactions.

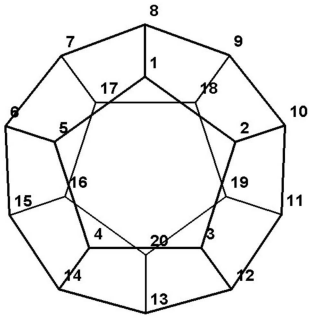

(a) $C_{20}H_{20}$ cages (hydrogen atoms deleted for clarity regarding carbon numbering)

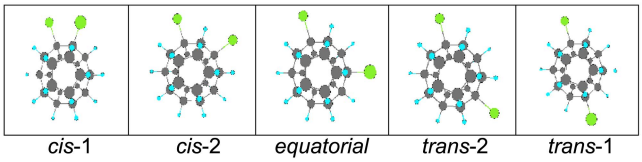

(b) Disubstituted $C_{20}H_{18}X_2$ cages

Figure 1. (a) $C_{20}H_{20}$ cluster cages. Hydrogen atoms are omitted to enable clear imaging of the carbon numbering scheme used to distinguish the different substituent sites. (b) The disubstituted regioisomers of $C_{20}H_{18}X_2$ cages where X = F, Cl, Br, or OH.

Calculations

In this study, the hybrid density-functional theory (DFT) with Becke's three-parameter hybrid method and the Lee-Yang-Parr exchange-correlation functional theory (B3LYP)[15-17] were used to optimize the geometries of the $C_{20}H_{20}$ and $C_{20}H_{18}X_2$ (X = F, Cl, Br, or OH) regioisomers. The electron basis set 6-31G(d,p) was used in this study.[18] We fully optimized the geometries of all the $C_{20}H_{18}X_2$ regioisomers using the Gaussian 2003 B.04 package suite.[19] To obtain highly-accurate geometries, we used the convergence criterion with tight optimization and an ultrafine pruned (99,590) grid (using the keywords Opt = Tight, Grid = ultrafine). We analyzed the relative energies and the HOMO and LUMO orbitals of the regioisomers.[20]

Table 2. The HOMO and LUMO energies (eV), the energy gap ($\Delta\varepsilon_g$) between the HOMO and LUMO energies, strain energies (kJ/mol), and the distance between the two substituents of $C_{20}H_{18}X_2$ (X = F, Cl, Br, or OH) regioisomers at the level of B3LYP/6-31G(d, p) calculations

$C_{20}H_{18}F_2$	Distance (Å)	HOMO (eV)	LUMO (eV)	$\Delta\varepsilon_g$ (eV)	Strain E (kJ/mol)
cis-1	2.521	-7.361	0.569	7.929	4.2
cis-2	4.108	-7.346	0.624	7.970	-6.3
equatorial	5.813	-7.366	0.630	7.996	-3.1
trans-2	6.649	-7.390	0.629	8.018	-4.4
trans-1	7.117	-7.365	0.635	7.999	-2.9
$C_{20}H_{18}Cl_2$					
cis-1	3.123	-7.350	-0.494	6.857	27.3
cis-2	4.637	-7.422	-0.390	7.033	-6.0
equatorial	6.556	-7.422	-0.250	7.173	-3.6
trans-2	7.504	-7.423	-0.264	7.159	-4.1
trans-1	8.034	-7.468	-0.218	7.250	-3.0
$C_{20}H_{18}Br_2$					
cis-1	3.307	-6.608	-1.005	5.603	17.1
cis-2	4.814	-6.957	-0.807	6.150	-12.1
equatorial	6.803	-6.966	-0.619	6.347	-8.3
trans-2	7.787	-6.972	-0.642	6.331	-9.4
trans-1	8.336	-7.012	-0.584	6.427	-7.7
$C_{20}H_{18}(OH)_2$					
cis-1	2.608	-6.622	0.821	7.443	20.1
cis-2	4.167	-6.591	0.837	7.428	9.9
equatorial	5.892	-6.577	0.841	7.418	9.8
trans-2	6.715	-6.615	0.839	7.454	10.5
trans-1	7.226	-6.614	0.842	7.457	10.2

Results and Discussion

By performing calculations for the full optimization of the atomic structures of the $C_{20}H_{18}X_2$ (X = F, Cl, Br, or OH) regioisomers at the level of B3LYP/6-31G(d,p) without any constraints, we determined the relative energies of the regioisomers with C_{2v} (*cis*-1), C_s (*cis*-2), C_2 (*equatorial*), C_{2v} (*trans*-2), and D_{3d} (*trans*-1) symmetries, as shown in Table

Table 1. Total energies (a.u.) and relative energies (in parentheses, in units of kJ/mol) of $C_{20}H_{18}X_2$ (X = F, Cl, Br, or OH) regioisomers. The energies were obtained through B3LYP/6-31G(d, p) calculations[a]

Regioisomers	$C_{20}H_{18}F_2$	$C_{20}H_{18}Cl_2$	$C_{20}H_{18}Br_2$	$C_{20}H_{18}(OH)_2$
cis-1 C_{2v}	-972.683481 15.1	-1693.399594 26.5	-5916.423368 23.5	-924.651855 0.0
cis-2 C_s	-972.688365 2.2	-1693.408233 3.8	-5916.430791 4.0	-924.646874 13.1
Equatorial C_2	-972.689029 0.5	-1693.409425 0.7	-5916.431951 1.0	-924.646438 14.2
trans-2 C_{2v}	-972.689066 0.4	-1693.409561 0.4	-5916.432118 0.5	-924.646309 14.6
trans-1 D_{3d}	-972.689218 0.0	-1693.409697 0.0	-5916.432315 0.0	-924.646454 14.2

[a]The relative energy of each regioisomer is the energy minus the lowest energy among the regioisomers.

1, under the reinforced tight convergence criterion. The cutoffs on the forces and step size are reduced by the pruned (99,590) grid (keywords Opt = Tight, Grid = ultrafine) used to obtain accurate geometries. The atomic structures, HOMOs, and LUMOs of the regioisomers of the different $C_{20}H_{18}X_2$ derivatives are shown in Figure 2. Further, we analyzed the effect of the disubstituents on the strain in the most-stable cage of neutral $C_{20}H_{20}$ with I_h symmetry (the calculated C-C bondlength is 1.556 Å, which is in the range of the corrected experimental result[21] 1.555 ± 0.003 Å), and we determined the strain energies of the regioisomers of each $C_{20}H_{18}X_2$ derivative, as shown in Table 2.

Although the dodecahedrane cage is formed of only pentagons, first principle calculations of the relative energies of the regioisomeric $C_{20}H_{18}X_2$ derivatives has not been performed, yet. Therefore, in this study, we considered five regioisomers for each $C_{20}H_{18}X_2$ derivative cage obtained by full geometry optimization. Among the five regioisomers whose geometries were fully optimized, the relative energies in the dihalide derivatives are dependent on the distance between the two halogen atoms but are independent of the type of symmetry. The relative energies of dihalo dodeca-

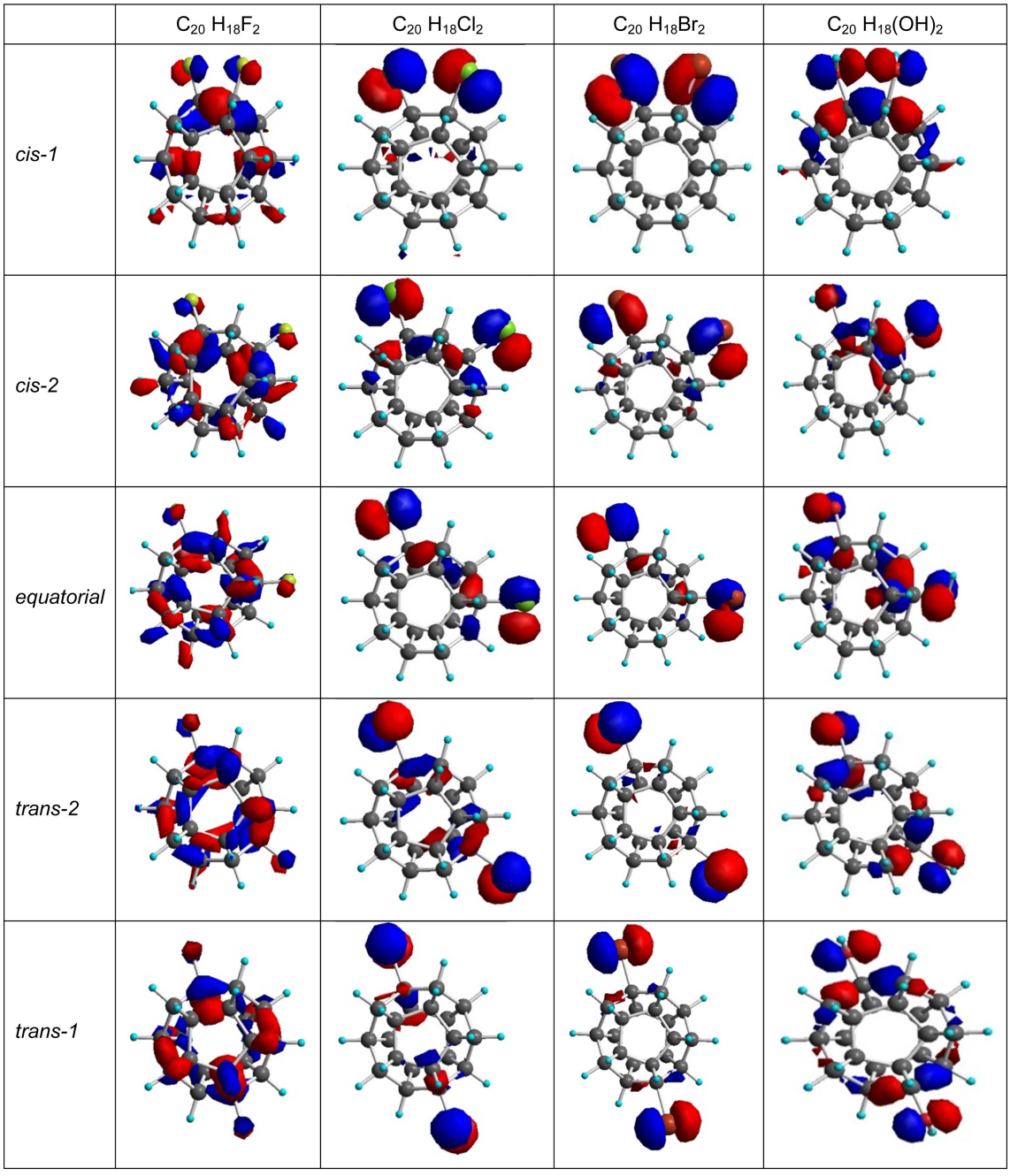

(a) The HOMOs of $C_{20}H_{18}X_2$ regioisomers (isovalue = 0.05)

Figure 2. The HOMOs (a) and LUMOs (b) of fully optimized geometries of five $C_{20}H_{18}X_2$ regioisomers at the level of B3LYP/6-31G(d, p). Here, X = F, Cl, Br, or OH. (c) The HOMO and LUMO of $C_{20}H_{20}$ cage at the level of B3LYP/6-31G(d, p)

	$C_{20}H_{18}F_2$	$C_{20}H_{18}Cl_2$	$C_{20}H_{18}Br_2$	$C_{20}H_{18}(OH)_2$
cis-1	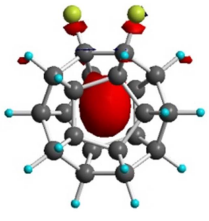	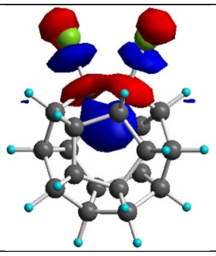	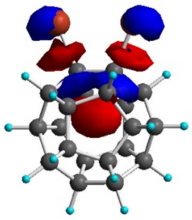	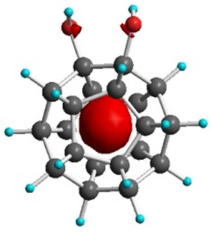
cis-2	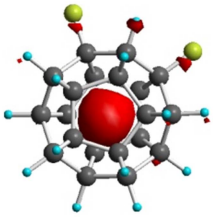	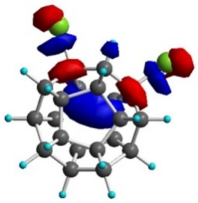	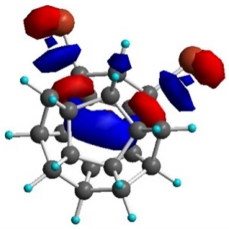	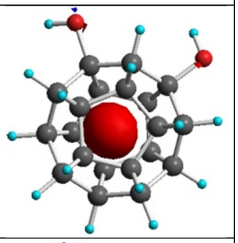
equatorial	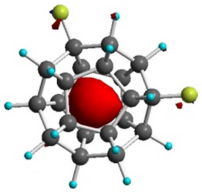	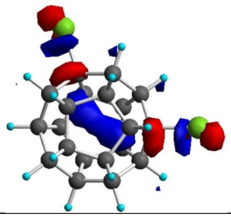	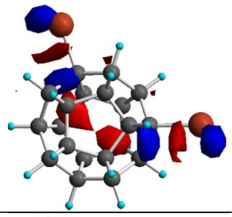	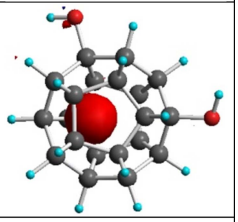
trans-2	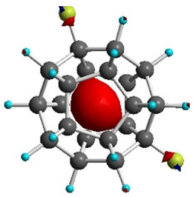	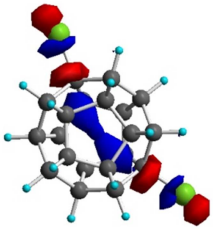	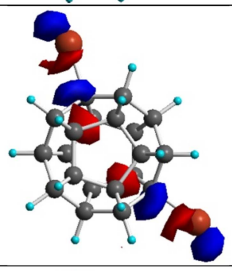	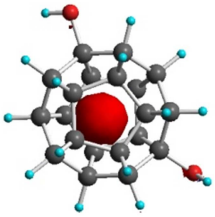
trans-1	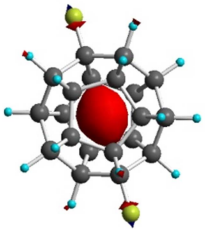	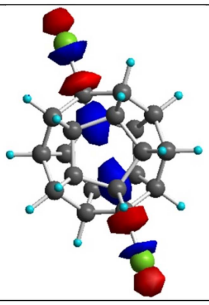	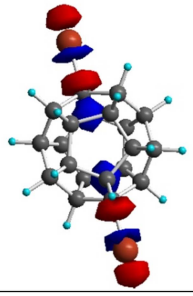	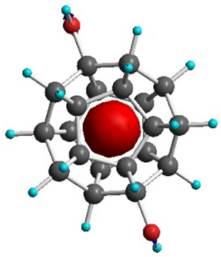

(b) The LUMOs of $C_{20}H_{18}X_2$ regioisomers (isovalue = 0.05)

	HOMO	LUMO
$C_{20}H_{20}$	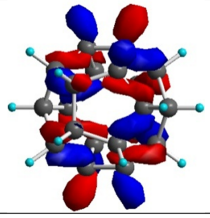	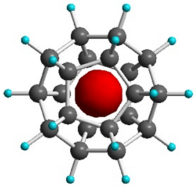

(c) The HOMO and LUMO of $C_{20}H_{20}$ cage (isovalue = 0.05)

Figure 2. Continued

heranes are in the following increasing order: *trans*-1 (D_{3d}) < *trans*-2 (C_{2v}) < *equatorial* (C_2) < *cis*-2 (C_s) < *cis*-1 (C_{2v}). Among these, the distance between the halides in the D_{3d} isomer (*trans*-1) with the lowest energy is the longest, and theses halides are the most symmetrical pair. It is interesting to compare with the case of $C_{20}X_2$(X=F, Cl, Br), in which *cis*-1 isomers have the lowest energy and *trans*-1 isomers have the highest energy.[25] The relative energies of the regioisomers of dihydroxy derivatives are in the following increasing order: *cis*-1 (C_{2v}) < *cis*-2 (C_s) < *equatorial* (C_2) < *trans*-2 (C_{2v}) < *trans*-1 (D_{3d}); the relative energies are proportional to the strength of the hydrogen bonds between the two hydroxyl groups. These support the experimental observation for *trans*-2 regioisomer of dihalo dodecahedranes and for vicinal diol *cis*-1 regioisomer of dihydroxy dodecahedrane.[22] Also in the atomic structures of the $C_{20}H_{18}X_2$, the calculated distance between nonbonding Br atoms for *trans*-2 (C_{2v}) is 7.787 Å, which agrees with the X-ray crystal structure of 7.728 Å.[6,22,23]

The calculated results showed that the strain energy of $C_{20}H_{20}$ due to pyramidalization of two carbon atoms of the cage is reduced by the substitution of F, Cl, or Br atoms in regioisomers (except in *cis*-1 isomers), while the strain energy is increased by the addition of OH groups in all five regioisomers. The fluorination of $C_{20}H_{20}$ is exothermic, but the chlorination, bromination, and hydroxylation reactions of $C_{20}H_{20}$ to yield all $C_{20}H_{18}X_2$ regioisomers are endothermic as follows:

$$C_{20}H_{20} + 2X \rightarrow C_{20}H_{18}X_2 + 2H \quad (1)$$

The reaction energy of the disubstituent reaction (1) for the synthesis of the *trans*-1 regioisomer (halogenation) and the *cis*-1 regioisomer (hydroxylation) is −102.1 kJ/mol in the case of fluorination, 294.1 kJ/mol in the case of chlorination, 273.1 kJ/mol in the case of bromination, and 48.9 kJ/mol in the case of hydroxylation.

Further, it is interesting that the *cis*-1 $C_{20}H_{18}(OH)_2$ cage with C_{2v} symmetry has the lowest energy, which indicates the existence of strong hydrogen bonds between the two hydroxyl groups because among the regioisomers, *cis*-1 $C_{20}H_{18}(OH)_2$ has the largest cage strain. Here the strain energy is calculated on the basis of the energy difference between the single point energies of the fragment $C_{20}H_{18}$ of optimized $C_{20}H_{18}X_2$ and the fragment $C_{20}H_{18}$ of optimized $C_{20}H_{20}$. However, our model calculations for the deformed cages of the $C_{20}H_{18}X_2$ regioisomers indicate that the dispersion interaction in dichloro and dibromo substitutions is a weaker affecting factor than the deformation strain of the naked cage is when the distance between the two substituents of the cage derivatives is approximately the same as the van der Waals distance. In the case of difloro substituion regioisomers, the dispersion interaction is competing to the cage strain effect. The computed distance between the two substituents in the *cis*-1 (C_{2v}) regioisomers is approximately equal to the van der Waals distance.[21] The most stable regioisomer was *trans*-1 with D_{3d} symmetry, followed by *trans*-2 (C_{2v}), equatorial (C_2), and *cis*-2 (C_s), and *cis*-1 (C_{2v}). Therefore, while the strength of the cage distortion are important factors affecting dihalogen substitution, the hydrogen bonds formed by dihydroxyl substitution are the strongest affecting component for the relative stability of the cage disubstituents (see Tables 1, 2 and S1-S9 in the supplementary material).

Figure 2 shows the HOMOs and LUMOs for the regioisomers of the $C_{20}H_{18}X_2$ disubstituents. Table 2 presents the strain energies and the energy gaps of the HOMO/LUMO energy levels of the regioisomers shown in Figure 2. Here, $C_{20}H_{20}$ and $C_{20}H_{18}X_2$ have different energy gaps, as shown in Table 2. Although the predominant electronic configurations of the $C_{20}H_{18}X_2$-disubstituent regioisomers with the same symmetry are similar, the HOMOs and LUMOs of regioisomers with different geometric structures are different. This suggests that the regioisomers undergo distinct set of characteristic chemical reactions. Figure 2 shows the effect of the disubstituents on the frontier orbitals of $C_{20}H_{20}$. The HOMO energies of $C_{20}H_{18}F_2$ and $C_{20}H_{18}Cl_2$ are decreasing, but the HOMO energies of $C_{20}H_{18}Br_2$ are increasing (compared to the HOMO of $C_{20}H_{20}$). The LUMO energy levels of all regioisomers are lower than that of $C_{20}H_{20}$ (HOMO: −7.087 eV; LUMO: 0.901 eV), in which the band gap is wider than that of C_{20} (HOMO: −5.034 eV; LUMO: −3.102 eV). In the case of all the $C_{20}H_{18}Cl_2$ and $C_{20}H_{18}Br_2$ regioisomers, the LUMO energies are negative and lower than that of $C_{20}H_{20}$, which implies that these are stronger electron acceptors than $C_{20}H_{20}$ is.

The HOMO and LUMO energy gaps of the equatorial, *trans*-2, and *trans*-1 regioisomers of $C_{20}H_{18}F_2$ are wider than that of $C_{20}H_{20}$; this trend is consistent with the fact that only the difluorination substitution is exothermic. In addition, the *cis*-1 and -2 regioisomers have narrower energy gaps, in which two substituents (except hydroxyl groups) are on the surface of the $C_{20}H_{20}$ fullerene within a distance equal to the van der Waals distance.

Conclusion

We obtained fully optimized geometries of the $C_{20}H_{18}X_2$ cage (the smallest fullerene disubstituents) without any constraint at the B3LYP/6-31G(d,p) level by the hybrid density-functional method for regioisomers. We observed that the relative energy of the $C_{20}H_{20}$ disubstituted regioisomers is mostly dependent on the distance between the two substituents. Therefore, it is interesting that the *cis*-1 regioisomer (1,2-dihalo derivatives) is less stable than the *trans*-1 (1,20-dihalo derivatives) regioisomer is, whereas in the case of the dihydroxy derivatives, the *cis*-1 regioisomer is more stable than the *trans*-1 regioisomer is. This implies that in the dihalo-induced strain cages of the $C_{20}H_{18}X_2$, the effect of the structural strain on the relative energy is crucial, while in the dihydroxide, the effect of the hydrogen bonds is stronger than that of the strain deformation. Here the regioisomer with vicinal substitution has the lowest energy in dihydroxide, but has the highest energy in dihalo dodecahedranes. Thus this supports the experimental result in which the

bisvicinal tetrol was of particular preparative-synthetic interest as a substitute for the lacking bisvicinal tetrabromide.

Although the predominant electronic configurations of the isomers are almost the same, the HOMO and LUMO maps of the five regioisomers of $C_{20}H_{18}X_2$ (X = F, Cl, Br, or OH) are different. Further, the topologies of the HOMO and LUMO characteristics of all $C_{20}H_{18}Cl_2$ and $C_{20}H_{18}Br_2$ regioisomers with the same symmetry are same, but they are different from those of $C_{20}H_{18}F_2$ and $C_{20}H_{18}(OH)_2$ regioisomers with the same symmetry. This suggests that the five regioisomers of the $C_{20}H_{20}$ disubstituted derivatives will have entirely different sets of characteristic chemical reactions, which could be verified empirically.

Supporting Information. Supplementary Tables S1-S9 are available at the BKCS website (http://www.kcsnet.or.kr/bkcs).

Acknowledgments. This study was supported by Wonkwang University in 2009.

References

1. Kroto, H. W. *Nature* **1987**, *329*, 529.
2. Schmalz, T. Z.; Seitz, W. A.; Klein, D. J.; Hite, D. G. *J. Am. Chem. Soc.* **1998**, *110*, 1113.
3. Prinzbach, H.; Weiler, A.; Landenberger, P.; Wahl, F.; Wörth, J.; Scott, L. T.; Gelmont, M.; Olevano, D.; Issendorff, B. von. *Nature* **2000**, *407*, 60.
4. Hirsch, A. *The Chemistry of Fullerenes*, New York: Thieme, 1994.
5. Sabirov, D. S.; Bulgakov, R. G.; Khursan, S. L. *Arkivoc* **2011**, *8*, 200.
6. Scheumann, K.; Sackers, E.; Bertau, M.; Leonhardt, J.; Hunkler, D.; Fritz, H.; Wörth, J.; Prinzbach, H. *J. Chem. Soc., Perkin Trans.* **1998**, *2*, 1195.
7. Prinzbach, H.; Wahl, F.; Weiler, A.; Landenberer, P.; Wörth, J.; Scott, L. T.; Gelmont, M.; Olevano, D.; Sommer, F.; Issendorff, B. von. *Chem. Eur. J.* **2006**, *12*, 6268.
8. Okamoto, Y. *Chem. Phys. Lett*. **2003**, *368*, 224.
9. Zhang, C.; Sun, W.; Cao, Z. *J. Chem. Phys.* **2007**, *126*, 144306.
10. Lee, J.; Lee, C.; Park, S. S.; Lee, K. H. *Bull. Korean Chem. Soc*. **2011**, *32*, 277.
11. Moran, D.; Simmonett, A. C.; Leach III, F. E.; Allen, W. D.; Schleyer, P. v. R.; Schaefer III, H. F. *J. Am. Chem. Soc.* **2006**, *128*, 9342.
12. An, Y.-P.; Yang, C.-L.; Wang, M.-S.; Ma, X.-G.; Wang, D.-H. *J. Phys. Chem. C* **2009**, *113*, 15756.
13. Irikura, K. K. *J. Phys. Chem. A* **2008**, *112*, 983.
14. Zhang, C.-Y.; Wu, H.-S.; Jiao, H. *J. Mol. Model* **2007**, *13*, 499.
15. (a) Beck, A. D. *J. Chem. Phys*. **1993**, *98*, 5648. (b) Lee, C.; Yang, W.; Parr, R. G. *Phys. Rev. A* **1988**, *37*, 785.
16. Stephen, P. J.; Devlin, F. J.; Chablowski, C. F.; Frisch, M. J. *J. Phys. Chem.* **1994**, *98*, 11623.
17. Herteing, R. H.; Koch, W. *Chem. Phys. Lett.* **1997**, *268*, 345.
18. Hehre, W. J.; Ditchfield, R.; Pople, J. A. *J. Chem. Phys.* **1972**, *56*, 2257.
19. Frisch, M. J. *et al*. A *Gaussian 03 B.04*, Gaussian, Inc., Pittsburgh, PA, 2003.
20. Clark, T. R.; Koch, R. *The Chemist's Electronic Book of Orbitals*; Springer-Verlag: Berlin, 1999.
21. Hudson, B. S.; Allis, D. G.; Parker, S. F.; Ramirez-Cuesta, A. J.; Herman, H.; Prinzbach, H. *J. Phys. Chem. A* **2005**, *109*, 3418.
22. Wahl, F.; Weiler, A.; Landenberger, P.; Sackers, E.; Voss, T.; Hass, A.; Lieb, M.; Hunkler, D.; Wörth, J.; Knothe, L.; Prinzbach, H. *Chem. Eur. J.* **2006**, *12*, 6255.
23. Sackers, E.; Oβwald, T.; Weber, K.; Keller, M.; Hunkler, D.; Wahl, F.; Wörth, J.; Knothe, L.; Prinzbach, H. *Chem. Eur. J.* **2006**, *12*, 6242.
24. Bond, A. *J. Phys. Chem.* **1964**, *68*, 441.
25. Lee, S.; Suh, Y.; Hwang, Y. G.; Lee, K. H. *Bull. Korean Chem. Soc*. **2011**, *32*, 3372.